Numerical and experimental study on hydrodynamic performance of multi-level OWEC

Sirirat Jungrungruengtaworn[1a], Ratthakrit Reabroy[*1],
Nonthipat Thaweewat[1b] and Beom-Soo Hyun[2c]

*[1]Department of Maritime Engineering, Faculty of International Maritime Studies,
Kasetsart University, Chonburi, Thailand*
*[2]Department of Naval Architecture and Ocean Systems Engineering,
Korea Maritime and Ocean University, Busan, Republic of Korea*

Abstract. The performance of a multi-level overtopping wave energy converter (OWEC) has been numerically and experimentally investigated in a two-dimensional wave tank in order to study the effects of opening width of additional reservoirs. The device is a fixed OWEC consisting of an inclined ramp together with several reservoirs at different levels. A particle-based numerical simulation utilizing the Lattice Boltzmann Method (LBM) is used to simulate the flow behavior around the OWEC. Additionally, an experimental model is also built and tested in a small wave flume in order to validate the numerical results. A comparison in energy captured performance between single-level and multi-level devices has been proposed using the hydraulic efficiency. The enhancement of power capture performance is accomplished by increasing an overtopping flow rate captured by the extra reservoirs. However, a noticeably large opening of the extra reservoirs can result in a reduction in the power efficiency. The overtopping flow behavior into the reservoirs is also presented and discussed. Moreover, the results of hydrodynamic performance are compared with a similar study, of which a similar tendency is achieved. Nevertheless, the LBM simulations consume less computational time in both pre-processing and calculating phases.

Keywords: wave energy; marine renewable energy; overtopping; LBM

1. Introduction

Oceans represent a substantial and predictable resource of renewable energy, e.g., tidal, wave, salinity gradient, and thermal energy. As a result, the ocean energy sources have a great advantage compared to other renewable energy sources. The share of ocean renewable energy in electricity generation is about 4% (Shadman *et al*. 2019). It has been reported that the global deployment potential of ocean energy is approximately 337 GW, and over 885 TWh of electricity can consequently be generated annually (de Andres *et al*. 2017). However, ocean energy technology has

∗Corresponding author, D.Eng., E-mail: ratthakrit.r@ku.th
[a] D.Eng., E-mail: sirirat.jun@ku.th
[b] Assistant professor, E-mail: nonthipat.t@ku.th
[c] Professor, E-mail: bshyun@kmou.ac.kr

been developed in slow progress compared to other renewable energy resources and has not yet in the commercialization stage (Melikoglu 2018). Thus, the present study intends to develop ocean wave energy technology suitable to the specific area and integrated with the breakwater function to prevent coastal erosion.

A device used to extract or harvest wave energy is called wave energy converter (WEC). The devices can be classified according to their characteristics, i.e., locations, orientations in wave, and working principles (Drew *et al*. 2009, López *et al*. 2013). The location can be classified into three categories: shoreline, nearshore, and offshore, while the orientation of wave energy devices can be classified into three predominant types: point absorber, attenuator, and terminator as schematically illustrated in Fig. 1. As for the working principle or operation mode, significant wave energy extraction concepts can be categorized, for examples: oscillating device (Cho *et al*. 2012, Cho and Kim 2013, Kim *et al*. 2019), oscillating water column (Koo and Kim 2012, Cui and Hyun 2016, Cui *et al*. 2017), and overtopping wave energy converter.

Among the large variation of ideas for wave energy extraction concepts, the overtopping wave energy converter (OWEC) is one of the most compelling approaches. This is because the device is capable of converting the relatively unstable wave energy into a considerably stable static form, i.e., steady potential energy through the stored water in a reservoir (Han *et al*. 2018). The working principle of OWEC is based on raising water into a reservoir area of the device. In order to practically achieve the mentioned energy conversion process, the OWEC has a sloping arm to lift waves overtop into a reservoir of which the stored water has the hydrostatic head greater than the surrounding sea level (Mustapa *et al*. 2017). Wave energy is therefore captured and accumulated in the form of potential energy of the stored water. The potential energy can be converted to mechanical energy via a turbine and subsequently transformed into electrical energy by a generator.

There are various of wave energy devices based on the overtopping concept. Typically, an OWEC device can exist in two types: floating and fixed. An example of the offshore floating OWEC type is the Wave Dragon, which consists of two wave reflectors focus on the incoming waves toward a ramp (Kofoed *et al*. 2006). Wave overtopping behavior of the Wave Dragon model was studied by a comparison between simulated flow and experimental data (Tedd and Kofoed 2009). It has been found that the results from the simulation supported the distribution of the measured overtopping flow rate. The survivability of Wave Dragon was tested on scale 1:50, which possesses excellent stability and energy absorption (Kofoed and Frigaard 1999, Sørensen *et al*. 2000). Moreover, the prototype model of Wave Dragon OWEC of 1:4.5 scale ratio was tested in Nissum Bredning, Denmark in 2003; the power capture performance was estimated around 23% with wave potential of 6 kW/m (Parmeggiani *et al*. 2011).

A fixed OWEC was developed in 1980. The device is a tapered channel wave power device, also known as TAPCHAN. The working concept of this device is similar to the conventional hydroelastic power plant technology (Evans and Antonio 2012). Another example of fixed OWEC is the Seawave Slot-cone Generator (SSG) which possesses several reservoirs at different crest levels. These multi-level reservoirs enable the device to efficiently capture wave power within a wide range of ocean conditions, e.g., tidal range and wave height. The power takeoff unit of SSG is typically a set of low head turbines (Margheritini *et al*. 2009). The crest level and geometrical layout of the SSG model were studied and optimized. The results have shown that, for a 3-level reservoir design, the overall hydraulic efficiency of the prototype can be over 40% for nearshore wave conditions (Kofoed and Osaland 2005). Moreover, the hydrodynamic force acting on SSG has been obtained by CFD simulation in order to investigate the magnitude and distribution of forces exerted on the surface on the SSG structure (Vicinanza *et al*. 2015, Buccino *et al*. 2019b, a). The width of opening slot of

(a) Point absorber   (b) Attenuator   (c) Terminator
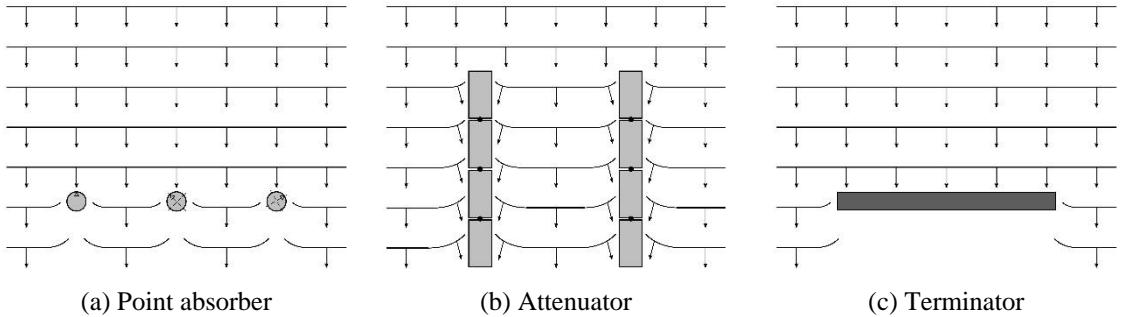
Fig. 1 Schematic illustration of WECs classified by their orientations in wave. The arrows indicate wave direction while the horizontal lines represent incident wavefront

reservoirs on the SSG structure was studied in a two-dimensional numerical tank (Jungrungruengtaworn and Hyun 2017, 2018). It has been shown that the optimal hydraulic efficiency is obtained at an intermediate value of the studied parameter. Other shape parameters, such as slope angles and gap height between reservoirs, have been numerically and experimentally studied (Han *et al*. 2018, Liu *et al*. 2018). Mostly, experiments or numerical simulations have been performed on the basis of two-dimensional phenomena.

Since the wave overtopping behavior around multi-level OWEC is highly complicated, an inappropriate setting can lead to completely different results between experimental and numerical methods. The present study therefore focuses on the comparison between the results obtained from experiments in a wave tank and numerical simulations using a particle-based CFD utilizing Lattice Boltzmann Method (LBM). Additionally, the results are compared with that of RANS method reported by a similar study. This paper is organized as follows: Section 1 presents the general research background in renewable energy status, ocean energy sources, and including WEC technology. The wave energy device and testing condition are described in Section 2, while Section 3 presents a numerical wave tank computation and optimization of scale resolution base on Lattice Boltzmann Method. The experimental setup for an experimental model in scale of 1:50 is explained in Section 4. The comparison result of capture width ratio and the overtopping behavior obtained by different methods are presented in Section 5. Finally, concluding remarks are given in Section 6.

2. Wave energy device

The wave energy device employed in this study is based on the overtopping principle, i.e., overtopping wave energy converter (OWEC). The baseline model is a single-level OWEC which is fixed stationary. The device consists of an inclined ramp in which the incident waves run-up and overtop into a single reservoir, as schematically illustrated in Fig. 2(a). The slope ratio S is defined as the ratio between the height R and length L of the entire ramp, which is $S = R/L$. The freeboard or crest height R_c and draught or submerged depth R_s are identical and fixed as 2 m measured vertically from the mean water level (MWL), while the horizontal length of the ramp is $L = 8$ m, yielding the slope ratio S of $1/2$ for both freeboard and draught parts.

In comparison with the single-level layout, the multi-level OWEC has 3 additional slots. These slots have a horizontal opening width of w allowing water wave flows into these extra reservoirs.
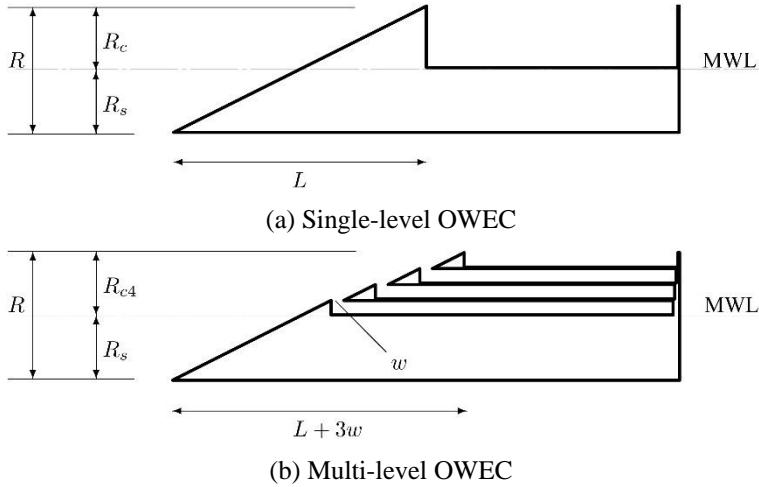
(a) Single-level OWEC

(b) Multi-level OWEC

Fig. 2 Design layouts of the single- and multi-level devices which are fixed stationary (Jungrungruengtaworn and Hyun 2017). The incident wave direction is from left to right

The crest height of the opening slots are $R_{c1} = 0.5$ m, $R_{c2} = 1.0$ m and $R_{c3} = 1.5$ m. The crest height of the main reservoir R_{c4} and the submerged depth R_s are fixed equivalent to that of single-level device. The slope ratio of multi-level device is defined only for the solid part of each discrete ramp as $S = R/L = 1/2$, in which the width of extra slots is not taken into account. The schematic illustration of the multi-stage layout is represented in Fig. 2(b).

In order to systematically study the influence of opening width w on the overtopping performance of the device, the parameter is therefore non-dimensionalized and is varied within the range of $0.0 \leq w/R_{c4} \leq 0.3$ with a 0.05 increment. Note that $w/R_{c4} = 0$ represents the single-level design. As for the numerical simulation, the generated linear wave or more precisely Airy wave possessing wave height $H = 2$ m together with wave period $T = 6$ s is utilized following a similar study (Jungrungruengtaworn and Hyun 2017). This consequently makes the results reasonably comparable.

Table 1 Ocean environment conditions

Parameters	Simulation	Experiment
Water depth, d [m]	20.0	0.4
Wave height, H [m]	2.0	0.04
Wave period, T [s]	6.0	0.849
Freeboard, R_{c4} [m]	2.0	0.04
Submerge depth, R_s [m]	2.0	0.04
Wave steepness, H/λ [-]	0.036	0.036
Relative freeboard, R_c/H [-]	1.0	1.0
Relative wave height, H/d [-]	0.1	0.1
Relative slot width, w/R_{c4} [-]	[0.05, 0.30]	[0.05, 0.30]

Due to the capability limitation of the laboratory facility, the scale of laboratory test has subsequently been set to 1:50 compared to the numerical simulation. This scale ratio is identical to the model experiments of the Wave Dragon conducted by Kofoed and Frigaard (1999). A dimensional analysis, based on Froude number and dispersion relation, is therefore performed for the experiment to achieve the flow similarity between the two methods. The wave and other testing conditions for both numerical and experimental methods are summarized in Table 1.

In a practical setting, the overall efficiency of an OWEC can be considered as a combination of partial efficiencies, i.e., hydraulic, reservoir, turbine and generator efficiencies. The first one indicates the capability in converting the unstable wave energy into a relatively stable static form, i.e., the potential energy of water stored in the reservoir. In the present study, only this process of energy conversion performance of the OWEC is considered and presented by the capture width ratio (CWR). This dimensionless number can be defined as

$$\text{CWR} = \frac{P_{crest}}{B \cdot P_{wave}} \tag{1}$$

where

$$P_{crest} = \sum_{i=1}^{n} Q_i \rho g R_{c,i} \tag{2}$$

and

$$P_{wave} = \frac{1}{8} \rho g H^2 \cdot c \cdot \frac{1}{2} \left[1 + \frac{2kd}{\sinh(2kd)} \right] = Ecn \tag{3}$$

where P_{crest} is the rate of overtopping energy flow into the reservoirs, Q_i is the time-averaged overtopping flow rate of the ith reservoir, ρ is the water density, g is the gravitational acceleration, $R_{c,i}$ is the crest height of the ith reservoir, H is the incident wave height, and d is the water depth. The parameter B is the span length of the wave energy device. This parameter is deliberately 1 m for the two-dimensional numerical simulation, while that of the experiment is 0.6 m which is the entire width of the flume. The wave power per unit crest width P_{wave} can be calculated from Eq. (3) (Xie and Zuo 2013) which consists of three variables: wave energy density E, phase velocity c, and factor n. The factor n depends mainly on the region of water depth: for deep water $n \approx 1/2$ and for shallow water $n \approx 1$.

3. Numerical tool

The numerical tool used to simulate the wave overtopping behaviour is a CFD solver based on the Lattice Boltzmann Method (LBM). This particle-based solver is provided by a commercial CFD simulation XFlow 2018 of Dassault Systèmes. Unlike the traditional CFD methods, this alternative approach uses statistical distribution function f_i to describe the collective behaviour of mesoscopic particles. These particles perform consecutively collision and streaming, or more precisely propagation, processes over discrete lattice nodes. The governing equation is the discrete
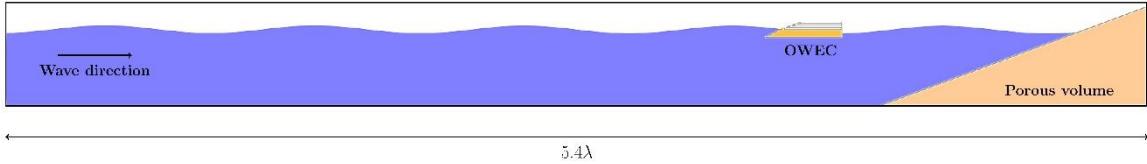
Fig. 3 The two-dimensional numerical wave tank used to simulate wave overtopping behavior. The ocean wave condition is given in Table 1

lattice Boltzmann equation

$$f_i\left(x+c_i\delta t,t+\delta t\right)=f_i\left(x,t\right)+\Omega_i\left(x,t\right) \tag{4}$$

where f_i is the particle distribution function for discrete direction i, c_i is the corresponding discrete velocity, and Ω_i is the collision operator. Macroscopic parameters, i.e., density ρ and momentum ρu, can be determined using the equilibrium distribution functions as

$$\rho=\sum_{i=0}^{b-1}f_i \tag{5}$$

and

$$\rho u=\sum_{i=0}^{b-1}f_ic_i \tag{6}$$

respectively, where *b* is the number of discrete directions of particle velocities. This LBM-based CFD solver naturally uses D3Q27 model with twenty seven velocities for three-dimensional flow. However, in this study, the lattice scheme model can be reduced as D2Q9 since the flow simulation is deliberately two-dimensional.

As for the collision operator, a Multiple Relaxation Time (MRT) collision scheme in central moment space is used in order to improve the Galilean invariance, numerical stability and accuracy (Lallemand and Luo 2000, 2003). The turbulence model used in this solver is the Large-Eddy Simulation (LES) approach. This consequently means that the turbulence at scales larger than the lattice node size is numerically resolved, while subgrid scales will be modeled. The mathematical model applied for turbulence closure and near-wall treatment is the wall-adapting local eddy (WALE).

The flow around wave energy device is numerically simulated in a two-dimensional domain with the length of 300 m roughly corresponding to 5.4λ, where λ is the wavelength, as shown in Fig. 3. A 1:3 slope ratio artificial beach modeled by a porous volume is placed at the right end of domain acting as wave absorber. In order to optimize the computational expense with a proper resolution, or more precisely the lattice node size, the sensitivity of scale resolution is investigated. The resolutions of far-field and wave absorber zone are always set to 2^{-2} m and 2^{-3} m respectively. To vary the lattice size from the far-field region to areas of interest, an adaptive refinement scheme is employed in the vicinity of both OWEC and free surface.
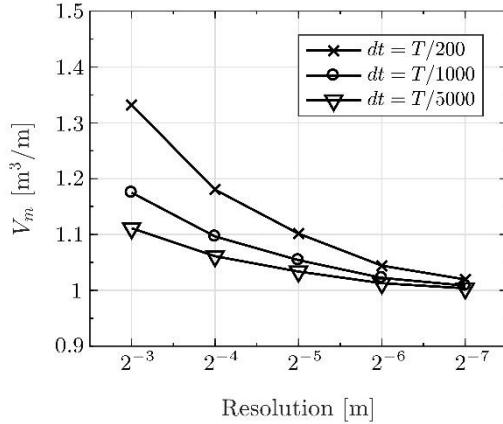
Fig. 4 Investigation of scale resolution and time-step size, V_m is the total fluid volume flow through the opening of the main reservoir, measured using different scale resolutions and time-step sizes

Table 2 Lattice node size

Region	Resolution [m]
Wave energy device	2^{-6}
Free surface	2^{-6}
Wave absorber	2^{-3}
Far-field	2^{-2}

A water volume of 1 m^3/m is imposed over the main reservoir and is released to freely fall-down. The total volume of water flow into the main reservoir V_m is measured at the crest level using different scale resolutions and time-step sizes. The investigation results are shown in Fig. 4. The lattice node size of 2^{-6} m is therefore deliberately utilized which is considered sufficient to capture the flow physics with acceptable accuracy. This is because the finer node size yields the nearly coincident discharge with the 2^{-6} m case, while a coarser resolution results in a noticeable deviation.

The applied scale resolutions for different regions are summarized in Table 2. As the results also suggest, the time-step of $dt = T/1000$ is chosen as the optimal time-step size since the discharge slightly changes with a smaller time-step.

4. Laboratory experiments

The experimental tests are conducted in a wave flume at the Faculty of International Maritime Studies, Kasetsart University. The flume is 8.0 m long and 0.6 m width, while the water depth is 0.4 m corresponding to 1:50 scale ratio in comparison with the numerical simulations. The testing conditions are summarized in Table 1. The desired incident wave is generated at one end of the flume using a paddle-type wavemaker which is precisely controlled by an AC servo motor. Wave probes have been placed in front of the OWEC model in order to monitor surface elevation. As for the

damping zone at another end of the flume, an artificial beach made of porous material is installed in order to eliminate wave reflection.

The components of the physical test model are made of acrylic plates as shown in Fig. 5 which can be easily modified to adaptively vary the studied shape parameter, i.e., opening slot width *w*. A small submersible pump is connected to each reservoir to release the stored water volume into an external storage tank. This leads to sufficient storage volume of the reservoirs for several wave periods. The time-averaged overtopping flow rate into each reservoir is then calculated directly from the measured water level in the corresponding external storage tank. This method is dissimilar to that of numerical simulations of which the captured water is released using pressure outlet condition at the bottom of each reservoir.

5. Results and discussions

The overall hydrodynamic performance of the OWEC is presented by the capture width ratio (CWR) and shown in Fig. 6(a), in which the result from a comparable study (Jungrungruengtaworn and Hyun 2017) using RANS is also given for verification. The results predicted by different approaches qualitatively agree with each other in spite of a slight deviation. The LBM-based simulations seem to slightly underestimate the overall CWR compared to the experimental investigation, while that of RANS simulations are slightly overestimated. Despite the mentioned deviation in the CWR predicted by different approaches, the results have a similar trend of which the peak CWR is obtained at an intermediate value of opening slot width, i.e., $w/R_{c4} = 0.15$ for both LBM and experiments, and $w/R_{c4} = 0.2$ for RANS.
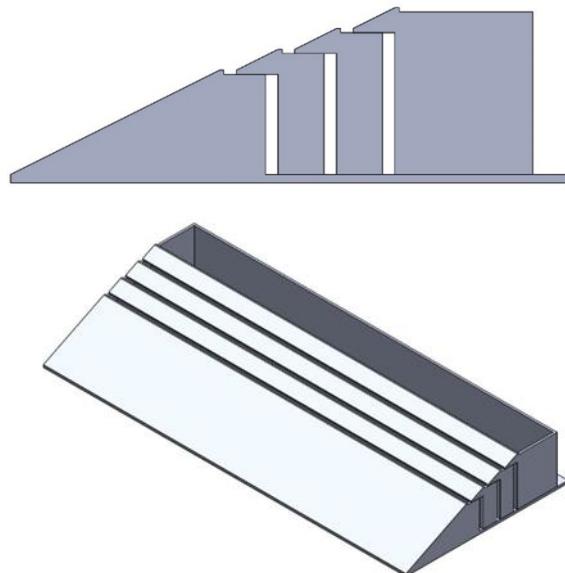

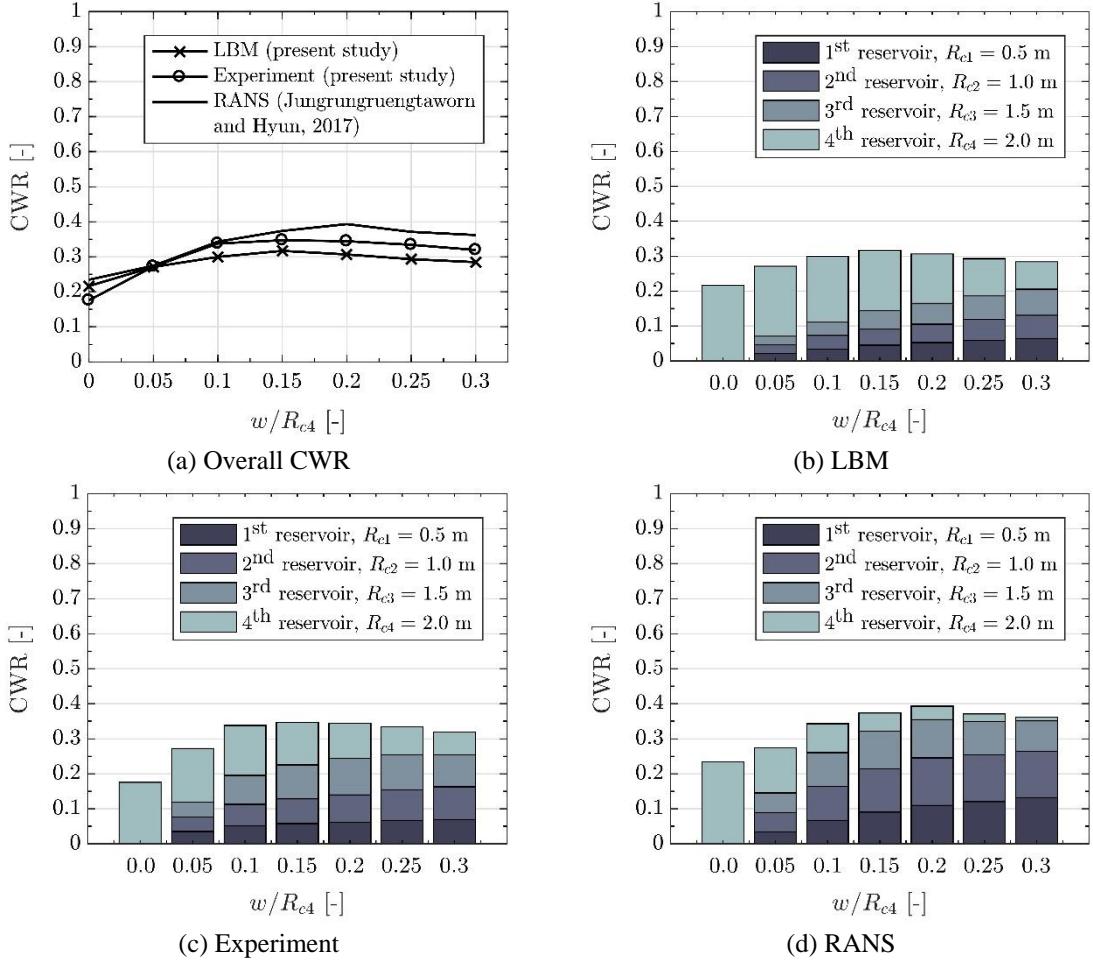Fig. 5 Components of the physical test model

Fig. 6 The CWR as a function of relative opening slot width: (a) overall CWR obtained from different methods; (b), (c), and (d) partial CWR achieved by LBM, experiment of 1:50 scale model, and RANS (Jungrungruengtaworn and Hyun 2017) respectively

The results also show a considerable enhancement in hydraulic efficiencies of about 30 - 40% for the multi-level model compared to 18 - 23% for the single reservoir layout ($w/R_{c4} = 0$). The results clearly demonstrate that the width of the opening slot has strong influence on the CWR performance of the OWEC device. This also confirms that the multi-level device is noticeably efficient and seemingly worthwhile approach in practice.

It should be pointed out that, although both time-step and mesh (or lattice node) sizes are optimized for the two numerical methods, the LBM takes approximately 5-6 times faster than the RANS as also consistently reported in literatures (Maroufi and Aghanajafi 2013, Chumchan and Rattanadecho 2020). The fact that LBM consumes less computational expenses while providing satisfactory accuracy especially for free surface problems makes the simulations practical on a normal personal computer, allowing preliminary analysis and possibly finding out the optimal design from more competitive layouts. Additionally, the LBM provides simplicity to study the

complex geometry since the method simplifies the meshing process generally used in the RANS simulations.

The bar charts in Fig. 6 represent CWR values versus the relative opening width w/R_{c4}. Each bar consists of the partial CWR values corresponding to all reservoirs. For the pre-peak regime, i.e., relatively small opening width, the overall hydraulic efficiency can be enhanced by increasing the studied parameter. The improvement of power capture performance is accomplished owing to the increase of overtopping flow rate captured and stored by extra reservoirs at lower crest heights during both run-up and fall-down processes. Nevertheless, when considering the main reservoir, the overtopping flow and wave capture performance is decreased since the lower reservoirs have partially collected and stored the water and wave energy. Moreover, when the slot width is further increasing, the overall efficiency is reduced, considering the wave energy is early captured and stored by the lower reservoirs. Subsequently, the upper reservoirs could slightly collect the remaining water with a small amount of energy. In other words, when the opening slot is wider, the greater volume of water is primarily stored by the lower reservoirs with the lower potential energy, while the higher reservoirs have less water being stored. Accordingly, this can illustrate the decrease of overall hydraulic efficiency caused by a relatively large opening slot of the extra reservoirs.

The behavior of overtopping flow into the reservoir is presented in Fig. 7 for both run-up and fall-down processes. The results predicted by LBM method are displayed in Figs. 7(a) and 7(b), which demonstrate that, in the run-up process, the overtopping flow mostly overtops into the main reservoir.

(a) Run-up (LBM)   (b) Fall-down (LBM)

(c) Run-up (Experiment)   (d) Fall-down (Experiment)

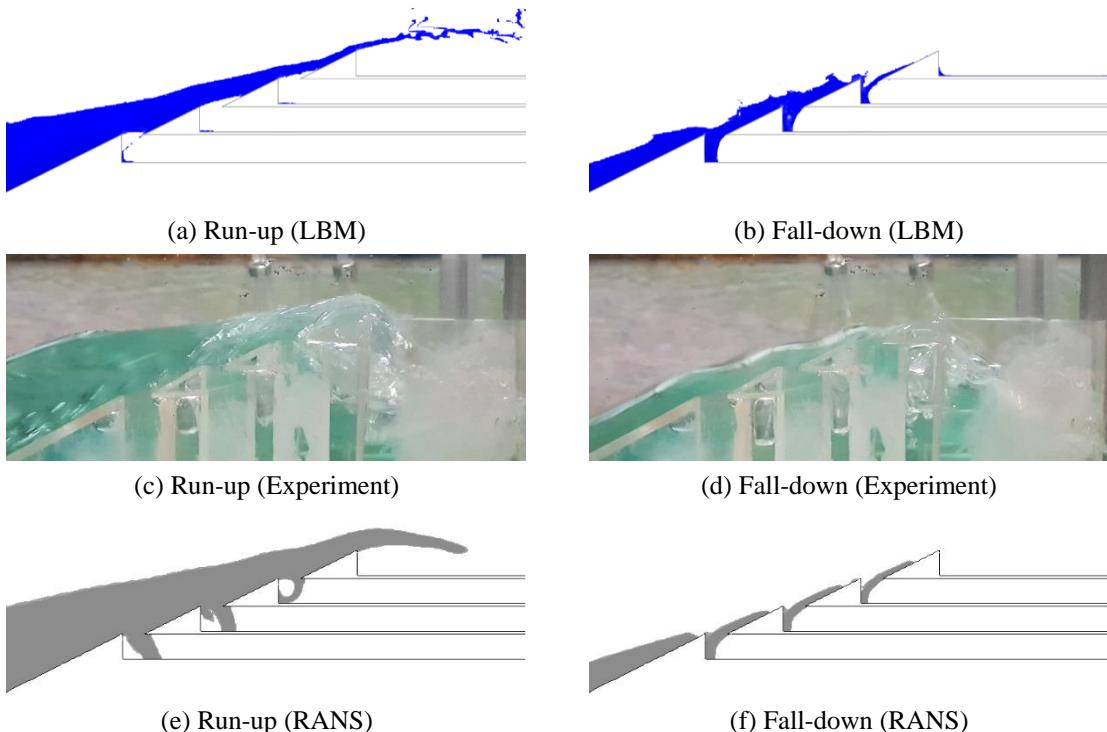(e) Run-up (RANS)   (f) Fall-down (RANS)

Fig. 7 Overtopping behavior achieved by different methods during both run-up (a), (c), (e) and fall-down (b), (d), (f). The relative opening slot width $w/R_{c4} = 0.2$

The extra reservoirs could capture the remaining water volume on the ramp mainly during the fall-down process. This explains why the CWR values of the LBM method exhibit the maximum in the main reservoir, which is similar to CWR results from the experiments within the entire range of parametric space considered, as shown in Figs. 6(b) and 6(c). In comparison with a similar study (Jungrungruengtaworn and Hyun 2017), the flow behaviors predicted using RANS (Figs. 7(e)-7(f)) are noticeably different as the overtopping water is captured by the extra reservoirs during both run-up and fall-down processes. This results in a small partial CWR of the main reservoir predicted by RANS as already mentioned and displayed in Fig. 6(d). The discrepancy in flow behavior between both numerical approaches has also be graphically reported in an investigation of dam break flow conducted by Chumchan and Rattanadecho (2020). It has been shown that the flow predicted by LBM could apparently maintain its momentum while passing through complex obstacles. On the other hand, the flow simulated by RANS seems to spread wider.

6. Conclusions

A set of numerical simulations and experiments has been conducted to investigate the effects of opening width of extra reservoirs on the performance of multi-level OWEC in stationary condition. It has been found that the LBM appears to simulate the overtopping behavior with satisfactory accuracy on performance predictions in spite of 5-6 times less computational expenses compared to RANS solver. The LBM also requires less effort and time spent in the meshing and pre-processing phase. It can subsequently be concluded that the particle-based CFD solver possesses reliability and accuracy which appears to be a computational tool suitable for free surface problems relevant to wave overtopping flow.

An optimal trend has been found for the hydraulic efficiency of which the peak performance is achieved at an intermediate value of the considered parameter. For a small value of the studied parameter, the extra reservoirs could appropriately capture the energy which slightly affects the wave run-up to the main reservoir. A relatively wider of the opening slot results in a greater volume of water stored by the extra reservoirs, yielding a significant reduction of the energy captured by the main reservoir. For the post-peak regime, the overall efficiency finally drops since the energy captured by the extra reservoirs could not worthily compensate for the decrease in energy captured by the main one. This tendency agrees well with the results reported by a similar study using different numerical method despite a slight deviation in the overall hydraulic efficiency.

A single-level OWEC possesses relatively low efficiency since it has only one reservoir at a certain level which is seemingly suitable for a specific range of sea wave conditions. This drawback could be resolved by the use of multi-level device consisting of several reservoirs at different crest levels which seems to perform efficiently over a wide range of ocean wave conditions. The multi-level layout therefore promises a more practical and feasible approach in practice compared to the single-level configuration. It is recommended to study the OWEC performance within a wider range of ocean conditions, i.e., tidal range, wave height and period. In order to further improve power capture performance, a hybrid configuration WEC, i.e., a combination concept between OWEC and OWC, will also be considered for future study.

Acknowledgments

References

Buccino, M., Daliri, M., Dentale, F. and Calabrese, M. (2019a), "CFD experiments on a low crested sloping top caisson breakwater. Part 2. Analysis of plume impact", *Ocean Eng.*, **173**, 345-357. https://doi.org/10.1016/j.oceaneng.2018.12.065.

Buccino, M., Daliri, M., Dentale, F., Leo, A.D. and Calabrese, M. (2019b), "CFD experiments on a low crested sloping top caisson breakwater. Part 1. Nature of loadings and global stability", *Ocean Eng.*, **182**, 259-282. https://doi.org/10.1016/j.oceaneng.2019.04.017.

Cho, I. and Kim, M. (2013), "Enhancement of wave-energy-conversion efficiency of a single power buoy with inner dynamic system by intentional mismatching strategy", *Ocean Syst. Eng.*, **3**(3), 203–217. https://doi.org/10.12989/ose.2013.3.3.203.

Cho, I., Kim, M. and Kweon, H. (2012), "Wave energy converter by using relative heave motion between buoy and inner dynamic system", *Ocean Syst. Eng.*, **2**(4), 297–314. https://doi.org/10.12989/ose.2012.2.4.297.

Chumchan, C. and Rattanadecho, P. (2020), "Experimental and numerical investigation of dam break flow propagation passed through complex obstacles using LES model based on FVM and LBM.", *Songklanakarin J. Sci. Technol.*, **42**(3), 564–572. https://doi.org/10.14456/sjst-psu.2020.71.

Cui, Y. and Hyun, B.S. (2016), "Numerical study on Wells turbine with penetrating blade tip treatments for wave energy conversion", *Int. J. Naval Architect. Ocean Eng.*, **8**(5), 456-465. https://doi.org/10.1016/j.ijnaoe.2016.05.009.

Cui, Y., Hyun, B.S. and Kim, K. (2017), "Numerical study on air turbines with enhanced techniques for OWC wave energy conversion", *China Ocean Eng.*, **31**(5), 517-527. https://doi.org/10.1007/s13344-017-0060-z.

de Andres, A., Medina-Lopez, E., Crooks, D., Roberts, O. and Jeffrey, H. (2017), "On the reversed LCOE calculation: Design constraints for wave energy commercialization", *Int. J. Marine Energy*, **18**, 88-108. https://doi.org/10.1016/j.ijome.2017.03.008.

Drew, B., Plummer, A. and Sahinkaya, M.N. (2009), "A review of wave energy converter technology", *Proceedings of the Institution of Mechanical Engineers, Part A: Journal of Power and Energy*, **223**(8), 887-902.

Evans, D.V. and Antonio, F.d.O. (2012), *Hydrodynamics of Ocean Wave-Energy Utilization: IUTAM Symposium Lisbon/Portugal 1985*, Springer Science & Business Media.

Han, Z., Liu, Z. and Shi, H. (2018), "Numerical study on overtopping performance of a multi-level breakwater for wave energy conversion", *Ocean Eng.*, **150**, 94-101. https://doi.org/10.1016/j.oceaneng.2017.12.058.

Jungrungruengtaworn, S. and Hyun, B.S. (2017), "Influence of slot width on the performance of multi-stage overtopping wave energy converters", *Int. J. Naval Architect. Ocean Eng.*, **9**(6), 668-676. https://doi.org/10.1016/j.ijnaoe.2017.02.005.

Jungrungruengtaworn, S. and Hyun, B.S. (2018), "Numerical Investigation of Design Strategy on Overtopping Performance of Multi-Stage OWEC", *Proceedings of the 2018 OCEANS - MTS/IEEE Kobe Techno-Oceans (OTO),* IEEE. https://doi.org/10.1109/oceanskobe.2018.8558884.

Kim, J., Cho, I.H. and Kim, M.H. (2019), "Numerical calculation and experiment of a heaving-buoy wave energy converter with a latching control", *Ocean Syst. Eng.*, **9**(1), 1-19. https://doi.org/10.12989/ose.2019.9.1.001.

Kofoed, J. and Frigaard, P. (1999), "Evaluation of hydraulic response of the Wave Dragon", *Test Report*.

Kofoed, J.P., Frigaard, P., Friis-Madsen, E. and Sørensen, H.C. (2006), "Prototype testing of the wave energy

converter wave dragon", *Renew. Energy*, **31**(2), 181-189. https://doi.org/10.1016/j.renene.2005.09.005.

Kofoed, J.P. and Osaland, E. (2005), "Crest level optimization of the multi level overtopping based wave energy converter seawave slot-cone generator", *Proceedings of the 6th European Wave and Tidal Energy Conference*, 243-250.

Koo, W. and Kim, M.H. (2012), "A time-domain simulation of an oscillating water column with irregular waves", *Ocean Systems Engineering*, **2**(2), 147–158. https://doi.org/10.12989/ose.2012.2.2.147.

Lallemand, P. and Luo, L.S. (2000), "Theory of the lattice Boltzmann method: Dispersion, dissipation, isotropy, Galilean invariance, and stability", *Physical Review E*, **61**(6), 6546.

Lallemand, P. and Luo, L.S. (2003), "Lattice Boltzmann method for moving boundaries", *J. Comput. Phys.*, **184**(2), 406-421. https://doi.org/10.1016/s0021-9991(02)00022-0.

Liu, Z., Han, Z., Shi, H. and Yang, W. (2018), "Experimental study on multi-level overtopping wave energy convertor under regular wave conditions", *Int. J. Naval Architect. Ocean Eng.*, **10**(5), 651-659. https://doi.org/10.1016/j.ijnaoe.2017.10.004.

López, I., Andreu, J., Ceballos, S., de Alegría, I.M. and Kortabarria, I. (2013), "Review of wave energy technologies and the necessary power-equipment", *Renew. Sust. Energy*, **27**, 413-434. https://doi.org/10.1016/j.rser.2013.07.009.

Margheritini, L., Vicinanza, D. and Frigaard, P. (2009), "SSG wave energy converter: Design, reliability and hydraulic performance of an innovative overtopping device", *Renew. Energy*, **34**(5), 1371-1380. https://doi.org/10.1016/j.renene.2008.09.009.

Maroufi, A. and Aghanajafi, C. (2013), "Analysis of conduction–radiation heat transfer during phase change process of semitransparent materials using lattice Boltzmann method", *J. Quantitative Spectroscopy Radiative Transfer*, **116**, 145-155. https://doi.org/10.1016/j.jqsrt.2012.10.019.

Melikoglu, M. (2018), "Current status and future of ocean energy sources: A global review", *Ocean Eng.*, **148**, 563-573. https://doi.org/10.1016/j.oceaneng.2017.11.045.

Mustapa, M., Yaakob, O., Ahmed, Y.M., Rheem, C.K., Koh, K. and Adnan, F.A. (2017), "Wave energy device and breakwater integration: A review", *Renew. Sust. Energy Review*, **77**, 43-58. https://doi.org/10.1016/j.rser.2017.03.110.

Parmeggiani, S., Chozas, J.F., Pecher, A., Friis-Madsen, E., Sørensen, H. and Kofoed, J.P. (2011), "Perfor mance assessment of the wave dragon wave energy converter based on the EquiMar methodology", *Proceedings of the 9th European Wave and Tidal Energy Conference (EWTEC)*, **9**.

Shadman, M., Silva, C., Faller, D., Wu, Z., de Freitas Assad, L., Landau, L., Levi, C. and Estefen, S. (2019), "Ocean renewable energy potential, technology, and deployments: A case study of Brazil", *Energies*, **12**(19), 3658. https://doi.org/10.3390/en12193658.

Sørensen, H., Hansen, R., Friis-Madsen, E., Panhauser, W., Mackie, G., Hansen, H., Frigaard, P., Hald, T., Knapp, W., Keller, J., Holmen, E., Holmes, B., Thomas, G. and Rasmussen, P. (2000), "The Wave Dragon: now ready for tests in real seas", *Proceedings of the 4th European Wave Energy Conference*, Aalborg, Denmark.

Tedd, J. and Kofoed, J.P. (2009), "Measurements of overtopping flow time series on the Wave Dragon, wave energy converter", *Renew. Energy*, **34**(3), 711-717. https://doi.org/10.1016/j.renene.2008.04.036.

Vicinanza, D., Dentale, F., Salerno, D., Buccino, M. *et al.* (2015), "Structural response of seawave slot-cone generator (SSG) from random wave CFD simulations", *Proceedings of the 25th International Ocean and Polar Engineering Conference*, International Society of Offshore and Polar Engineers.

Xie, J. and Zuo, L. (2013), "Dynamics and control of ocean wave energy converters", *Int. J. Dynam. Control*, **1**(3), 262-276. https://doi.org/10.1007/s40435-013-0025-x.

MK